Low-Overhead Iterative Channel Parameter Estimation for Multi-User OAM Wireless Backhaul

Wen-Xuan Long, *Member, IEEE*, Nian Li, *Graduate Student Member, IEEE*, Yuan Liu, *Graduate Student Member, IEEE*, M. R. Bhavani Shankar, *Senior Member, IEEE*, and Rui Chen, *Member, IEEE*

***Abstract*—This paper considers the issue of acquiring channel state information (CSI) for multi-user orbital angular momentum (MU-OAM) wireless backhaul between the macro base station (MBS) and small base stations (SBSs) within broadcasting networks. Unlike prior works, we assume that each SBS transmits a pilot signal of length one on each multiplexed OAM mode and subcarrier, resulting in the coherent observations collected at the MBS. Then, we construct the data sets using the coherent observations, the components of which independently contain arbitrarily assumed positional information. The amplitude-phase multiple signal classification (AP-MUSIC) algorithm, a novel variant of the MUSIC, then conducts a two-dimensional (2-D) search on the amplitude and phase of the data component in both the OAM mode and frequency domains for estimating positions at each iteration. These estimates, together with the observations, are used to iteratively update the data sets, ultimately refining the distances and AoAs of all SBSs. The theoretical analysis and simulation results indicate that this solution not only yields the precise CSI for the MU-OAM system, but also markedly reduces the training overhead, compared to existing alternatives.**

***Index Terms*—Broadcasting system, orbital angular momentum (OAM), angle of arrival (AoA) estimation, multiple signal classification (MUSIC).**

I. Introduction

THE SURGE in media data challenges the next-generation broadcasting networks [1], necessitating advancements in data rates, reliability and coverage. Heterogeneous networks, incorporating technologies such as multiple-input multiple-output (MIMO) [2], distributed caching [3] and network slicing [4], stand at the forefront of promising solutions to enhance data throughput and extend coverage in broadcasting networks. The heterogeneous network, as depicted in Fig. 1, is typically composed of a macro base station (MBS) layer and a small base station (SBS) layer [5], with backhaul connections between MBS and SBSs utilizing either wired or wireless methods. Given the deployment costs and widespread use of small cells, the wireless backhaul [6], [7] becomes the preferred method for connecting MBS and SBSs.

The orbital angular momentum (OAM) [8], characterized by orthogonal helical wavefront phases in space, presents a promising approach for wireless backhaul with high spectral efficiency (SE) between MBS and SBSs [9]. Specifically, the wavefront phase of an OAM-carrying wave rotates with the azimuth φ, resulting in a helical phase structure $e^{i\ell\varphi}$ in space, where ℓ is an integer that denotes the degree and direction of the wavefront's twist, referred to as the *OAM mode*. The orthogonality of wavefront phases across different OAM modes introduces a unique form of angular diversity in space, thereby providing an additional degree of freedom for information transmission [8], [9], [10]. This capability enhances the potential of OAM technology for high SE wireless backhaul.

The high SE multi-user OAM (MU-OAM) wireless backhaul hinges on the precise alignment between transmitted and received OAM beams. This alignment necessitates accurate channel state information (CSI), which is fundamentally determined by the relative distances and angles of arrival (AoA) between the MBS and SBSs [9], [10]. While the multi-user distance and AoA estimation for plane waves have been well-explored, extending these methods to accommodate MU-OAM scenarios remains a significant challenge. To date, only our preliminary investigations [9], [11] have addressed this issue. In [9], after collecting a substantial number of training samples across the OAM mode and frequency domains, the conventional FFT method was applied to extract the positions of all SBSs. Moreover, [11] utilized the recursive estimation of signal parameters via rotational invariance techniques (ESPRIT) algorithm for super-resolution AoA estimation of the SBSs. This technique, however, necessitates that all SBSs transmit pilot signals of a certain duration on each multiplexed OAM mode to ensure the signals remain uncorrelated when reaching the MBS, thereby incurring considerable training overhead. Additionally, developing a method for accurate multi-user distance estimation to obtain complete CSI remains an unresolved challenge as highlighted in [11].

Manuscript received 15 May 2024; accepted 3 July 2024. The work of Wen-Xuan Long, Nian Li, and Rui Chen was supported in part by the National Natural Science Foundation of China under Grant 62271376. The work of Yuan Liu and M. R. Bhavani Shankar was supported in part by the Luxembourg National Research Fund (FNR) through the BRIDGES Project MASTERS under Grant BRIDGES2020/IS/15407066, and in part by the CORE Project SENCOM under Grant C20/IS/14799710. *(Corresponding author: Wen-Xuan Long.)*

Wen-Xuan Long is with the Dipartimento di Ingegneria dell'Informazione, University of Pisa, 56126 Pisa, Italy, and also with the State Key Laboratory of Integrated Service Networks, Xidian University, Xi'an 710071, China (e-mail: wen-xuan.long@phd.unipi.it).

Nian Li and Rui Chen are with the State Key Laboratory of Integrated Service Networks, Xidian University, Xi'an 710071, China (e-mail: nianli@stu.xidian.edu.cn; rchen@xidian.edu.cn).

Yuan Liu and M. R. Bhavani Shankar are with the Interdisciplinary Center for Security, Reliability and Trust, University of Luxembourg, 4365 Esch-sur-Alzette, Luxembourg (e-mail: yuan.liu@uni.lu; bhavani.shankar@uni.lu).

Digital Object Identifier 10.1109/TBC.2024.3434676

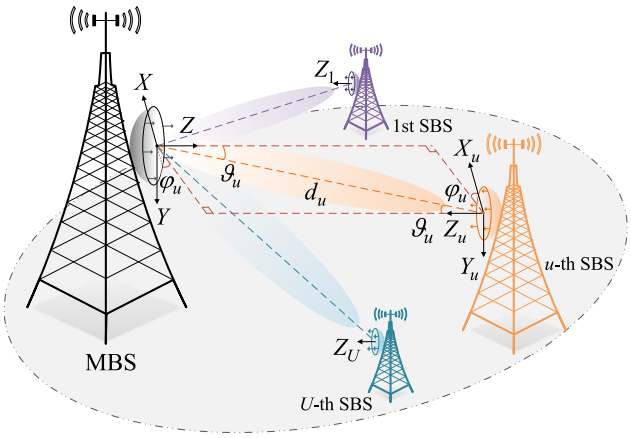

Fig. 1. The geometrical model of the transmit and receive UCAs in the downlink MU-OAM wireless backhaul system.

To address the above challenges, we present a novel iterative estimation method based on the amplitude-phase (AP)-MUSIC algorithm, to precisely estimate the distances and AoAs of all the SBSs. Initially, under the assumption that each SBS transmits a pilot signal of length $L = 1$ on each OAM mode and subcarrier, we create the data sets based on the coherent observations received by the MBS, whose components independently carry arbitrarily assumed positional information. Inspired by the MUSIC algorithm [12], we then develop a novel search vector during each iteration. This vector conducts a two-dimensional (2-D) search on both the amplitude and phase of the data component in both the OAM mode and frequency domains, termed as AP-MUSIC algorithm, yielding estimates of distances and AoAs at each iteration. These estimates, combined with the observations, are used to iteratively update the data sets, ultimately refining the distances and AoAs of all SBSs. Compared to the existing method [11], this approach 1) minimizes the required training overhead by eliminating the need for continuous transmission of pilot signals on multiplexed OAM modes and frequencies; 2) achieves high-precision distance and AoA estimation for SBSs using an advanced variant of the MUSIC algorithm, thereby facilitating the acquisition of exact CSI for MU-OAM wireless backhaul.

II. UCA-Based Multi-User OAM Wireless Backhaul System

We consider the MU-OAM wireless backhaul between a single MBS and U SBSs. Considering the feasibility of using uniform circular arrays (UCA) to generate and receive radio OAM beams, the antennas of the MBS are deployed as an UCA with P elements and the radius R_m, and each SBS is composed of Q antennas, also forming a UCA with the radius R_s. In the proposed system, there is off-axis misalignment between the arrays of the MBS and SBSs [9], [11], as shown in Fig. 1. Specifically, the UCA planes of the MBS and SBSs are parallel to each other, while the UCA centers of U SBSs are not coaxial. In the geometric model as shown in Fig. 1, the UCA center of the u-th SBS is defined as $(d_u, \vartheta_u, \varphi_u)$ in the coordinate system Z-XOY at the MBS. Based on the off-axis misalignment geometric relationship, the UCA center of the MBS can be expressed as $(d_u, \vartheta_u, \varphi_u + \pi)$ in $\mathrm{Z}_u - \mathrm{X}_u\mathrm{O}_u\mathrm{Y}_u$ at the u-th SBS, where d_u is the distance between the UCA centers of the u-th SBS and MBS, $\vartheta_u \in [-\pi/2, \pi/2]$ and $\varphi_u \in [0, 2\pi]$ are the elevation and azimuth angles, respectively, of the UCA center of the u-th SBS in Z-XOY. In this paper, we define $\{(\vartheta_u, \varphi_u)\}$ as the AoAs of the OAM beams from U SBSs.

The MU-OAM wireless backhaul operates according to a communication protocol [9] wherein the data transmission phase is preceded by a training phase. During the training phase, the MBS is required to perform multi-user distance and AoA estimation to obtain the exact CSI [9], [11]. To provide the range-angle-dependent training samples, we consider an OAM-OFDM-based signalling scheme [9], [13], where $M(M \le Q)$ OAM modes and N subcarriers are multiplexed. Then, U SBSs transmit the training sequences$\{\mathbf{s}_u \in \mathbb{C}^L | u = 1, \ldots, U\}$ of length L to the MBS on each OAM mode at each subcarrier. When arriving at an arbitrary point $A(d, \vartheta, \varphi)$ in the far-field of the u-th SBS, the signals transmitted by the u-th SBS on the m-th OAM mode at the n-th subcarrier takes the form[1]

$$\begin{aligned}
&\mathbf{e}_u(\mathbf{d}, \ell_m, k_n) \\
&= -j\frac{\mu_0\omega_n}{4\pi}\sum_{q=1}^{Q}\mathbf{s}_u \cdot e^{i\ell_m\phi_q^u}\int |\mathbf{d} - \mathbf{d}_q^u|^{-1} e^{ik_n|\mathbf{d}-\mathbf{d}_q^u|} dV_q \\
&\approx -j\frac{\mu_0\omega_n D}{4\pi}\frac{e^{ik_n d}}{d}\sum_{q=1}^{Q}\mathbf{s}_u \cdot e^{-i\left(\mathbf{k}_n\cdot\mathbf{d}_q^u - \ell_m\phi_q^u\right)} \\
&\approx -j\frac{\mu_0\omega_n DQ e^{ik_n d} e^{i\ell_m\varphi}}{4\pi d} i^{-\ell_m} J_{\ell_m}(k_n R_s \sin\vartheta)\cdot\mathbf{s}_u, \qquad (1)
\end{aligned}$$

where $\mathbf{d}$ is the position vector of the point $A(d, \vartheta, \varphi)$, i is the imaginary unit, j is the current density of the dipole, μ_0 is the magnetic conductivity in the vacuum, ω_n is the circular frequency, D is the electric dipole length, $\mathbf{k}_n$ is the wave vector and $k_n = |\mathbf{k}_n| = 2\pi f_n/c$ is the wave number corresponding to subcarrier frequency f_n, c is the speed of light in a classical vacuum, $\mathbf{s}_u = [s_u^1, \ldots, s_u^L]^{\mathrm{T}}$ is the training sequence of length L sent by the u-th SBS, $J_{\ell_m}(\cdot)$ is the ℓ_mth-order Bessel function of the first kind, $\phi_q^u = \frac{2\pi(q-1)}{Q}$ is the azimuth angle of the q-th UCA element in the u-th SBS, $\mathbf{d}_q^u = R_s(\mathbf{x}_u\cos\phi_q^u + \mathbf{y}_u\sin\phi_q^u)$, $\mathbf{x}_u$ and $\mathbf{y}_u$ are the unit vectors of X_u-axis and Y_u-axis, respectively.

The training samples received by each UCA element at the MBS are combined, thus yielding [9], [11]

$$\begin{aligned}
\mathbf{y}(\ell_m, k_n) &= \sum_{p=1}^{P}\sum_{u=1}^{U}\mathbf{e}_u(\mathbf{d}_u, \ell_m, k_n) + \mathbf{z}(\ell_m, k_n) \\
&\approx -j\frac{\mu_0\omega_n DPQ}{4\pi} i^{-\ell_m}\sum_{u=1}^{U}\mathbf{s}_u\frac{e^{ik_n d_u}}{d_u}e^{i\ell_m\varphi_u}\cdot \\
&\quad J_{\ell_m}(k_n R_s\sin\vartheta_u)J_0(k_n R_m\sin\vartheta_u) + \mathbf{z}(\ell_m, k_n), \qquad (2)
\end{aligned}$$

[1]The additional phase term related to the time slots is omitted in (1) under the assumption of a flat fading channel model per subcarrier.

where $\mathbf{d}_u$ is the position vector of $\mathrm{O}_u(d_u, \vartheta_u, \varphi_u)$ in Z-XOY, and $\mathbf{z}(\ell_m, k_n) \sim \mathcal{N}_{\mathbb{C}}(\mathbf{0}_L, \xi^2\mathbf{I}_L)$ is the additive white Gaussian noise. Then, the combined signals received on M OAM modes at N subcarriers are collected in a 3-D matrix $\mathbf{Y} \in \mathbb{C}^{M\times N\times L}$.

III. Channel Parameter Estimation Based on Coherent Observations

A. Problem Formulation

After compensating for the known constant terms unrelated to the distances and AoAs of U SBSs, the combined signals in (2) can be written as

$$\mathbf{y}'(\ell_m, k_n) = \sum_{u=1}^{U} \mathbf{s}_u \cdot \frac{e^{ik_n d_u}}{d_u} e^{i\ell_m\varphi_u} J_{\ell_m}(k_n R_s \sin\vartheta_u) \cdot J_0(k_n R_m \sin\vartheta_u) + \mathbf{z}'(\ell_m, k_n), \tag{3}$$

where $\mathbf{z}'(\ell_m, k_n) \sim \mathcal{N}_{\mathbb{C}}(\mathbf{0}_L, \frac{16\pi^2}{(j\mu_0\omega_n DPQ)^2}\xi^2\mathbf{I}_L)$. All the combined signals in $\mathbf{Y}$ are processed to yield $\mathbf{Y}' \in \mathbb{C}^{M\times N\times L}$.

From (3), the azimuth angle φ_u is closely associated with the OAM mode ℓ_m, through the exponential term $e^{i\ell_m\varphi_u}$, and the distance d_u and wave number k_n are similarly related. The elevation angle ϑ_u is related to both ℓ_m and k_n due to its presence in the amplitude $J_{\ell_m}(k_n R_s \sin\vartheta_u) J_0(k_n R_m \sin\vartheta_u)$. Therefore, we propose to estimate $\{(\vartheta_u, \varphi_u)\}$ by processing $\{\mathbf{Y}'(:, n, :) \in \mathbb{C}^{M\times L} | n = 1, \ldots, N\}$, whose columns depend on OAM modes. Similarly, the estimates $\{(\hat{d}_u, \hat{\vartheta}_u)\}$ can be obtained by processing $\{\mathbf{Y}'(m, :, :) \in \mathbb{C}^{N\times L} | m = 1, \ldots, M\}$. To simplify the following discussion, we assume $\triangle\ell = \ell_{m+1} - \ell_m = 1$ and $\triangle k = k_{n+1} - k_n = 1$ here.

Specifically, taking the processing in the OAM mode domain as an example, $\mathbf{Y}'(:, n, :)$ can be expressed in a compact form as

$$\mathbf{Y}'(:, n, :) = \tilde{\mathbf{Y}}'_n = \tilde{\mathbf{A}}_n \tilde{\mathbf{S}}_n + \tilde{\mathbf{Z}}_n, \tag{4}$$

where $\tilde{\mathbf{A}}_n = [e^{i\ell_m\varphi_u} J_{\ell_m}(k_n R_s \sin\vartheta_u)]_{M\times U}$ contains the AoA information of all SBSs carried in the OAM mode domain, $\tilde{\mathbf{S}}_n = \tilde{\Theta}_n \mathbf{S}$, $\tilde{\Theta}_n = \mathrm{diag}\{J_0(k_n R_m \sin\vartheta_1) e^{ik_n d_1}/d_1, , \ldots, J_0(k_n R_m \sin\vartheta_U) e^{ik_n d_U}/d_U\}^{\mathrm{T}}$, $\mathbf{S} = [\mathbf{s}_1^{\mathrm{T}}; \cdots; \mathbf{s}_U^{\mathrm{T}}]$. In our previous research [11], it is assumed that the training signals from U SBSs are uncorrelated upon arrival at the MBS, meaning that $\tilde{\mathbf{R}}_S^n = \mathbb{E}\{\tilde{\mathbf{S}}_n \tilde{\mathbf{S}}_n^{\mathrm{H}}\} = \tilde{\Theta}_n \mathbb{E}\{\mathbf{S}\mathbf{S}^{\mathrm{H}}\} \tilde{\Theta}_n^{\mathrm{H}}$ is a full-rank matrix. To ensure this, the training sequence length L sent by SBSs on each OAM mode (and at each subcarrier) is greater than U, resulting in significant training overhead. To minimize channel uses during the training phase, in the following, all SBSs are set only transmitting one training symbol $\{s_u\}$ of length $L = 1$ on each OAM mode (and at each subcarrier), which results in the matrix $\mathbf{Y}'$ degenerating into a 2-D matrix:

$$\mathbf{Y}' = \begin{bmatrix} y'(\ell_1, k_1) & \cdots & y'(\ell_1, k_N) \\ \vdots & \ddots & \vdots \\ y'(\ell_M, k_1) & \cdots & y'(\ell_M, k_N) \end{bmatrix}, \tag{5}$$

and N columns of $\mathbf{Y}'$:

$$\tilde{\mathbf{y}}'_n = \tilde{\mathbf{A}}_n \tilde{\mathbf{s}}_n + \tilde{\mathbf{z}}_n = \tilde{\mathbf{A}}_n \tilde{\Theta}_n \mathbf{s} + \tilde{\mathbf{z}}_n, n = 1, 2, \ldots, N \tag{6}$$

becoming the coherent observations, and $\mathbf{s} = [s_1, \ldots, s_U]^{\mathrm{T}}$.

The key in obtaining the estimates $\{(\hat{\vartheta}_u, \hat{\varphi}_u)\}$ from the coherent observation $\tilde{\mathbf{y}}'_n$ in (6) is to obtain the 'complete' data $\tilde{\mathbf{x}}_n$ that independently carries AoA information for U SBSs. A natural choice for $\tilde{\mathbf{x}}_n$ is obtained by decomposing the observation $\tilde{\mathbf{y}}'_n$ into its U signal components [14], namely,

$$\tilde{\mathbf{x}}_n = \left[\tilde{\mathbf{x}}_{n,1}^{\mathrm{T}}, \tilde{\mathbf{x}}_{n,2}^{\mathrm{T}}, \ldots, \tilde{\mathbf{x}}_{n,U}^{\mathrm{T}}\right]^{\mathrm{T}}, \tag{7}$$

with the u-th component given by

$$\tilde{\mathbf{x}}_{n,u} = \tilde{\mathbf{A}}_n(:, u)\tilde{\mathbf{s}}_n(u) + \beta_u \left[\tilde{\mathbf{y}}'_n - \sum_{u=1}^{U} \tilde{\mathbf{A}}_n(:, u)\tilde{\mathbf{s}}_n(u)\right], \tag{8}$$

where the former term is determined by the position $(d_u, \vartheta_u, \varphi_u)$ to be estimated for the u-th SBS, while the latter term is obtained by decomposing the noise $\tilde{\mathbf{z}}_n$ into U components arbitrarily, thus we have $\sum_u \beta_u = 1$. Due to the fact that the m-th element $[\tilde{\mathbf{x}}_{n,u}]_m$ in (8) (also in (7)) is a function of unknown positions, i.e.,

$$\left[\tilde{\mathbf{x}}_{n,u}\right]_m = \frac{e^{ik_n d_u}}{d_u} e^{i\ell_m\varphi_u} J_{\ell_m}(k_n R_s \sin\vartheta_u) J_0(k_n R_m \sin\vartheta_u) s_u + z'_u(\ell_m, k_n), \tag{9}$$

it is difficult to achieve the direct decomposition of $\tilde{\mathbf{y}}'_n$ into U-dimensional complete data $\tilde{\mathbf{x}}_n$. From the rows of $\mathbf{Y}'$, the same conclusion also holds for the vectorized observation $\check{\mathbf{y}}'_m$ and the complete data $\check{\mathbf{x}}_m$ in the frequency domain.

B. Iterative Estimation for $\{(d_u, \vartheta_u, \varphi_u)\}$

To address the above issue, an iterative estimation strategy can be adopted here, especially useful for handling incomplete data. Specifically, the initial data $\{\tilde{\mathbf{x}}_n^0\}$ (and $\{\check{\mathbf{x}}_m^0\}$) is determined by the assumed positions of U points arbitrarily. Then, at the w-th iteration, the data $\{\tilde{\mathbf{x}}_n^w\}$ (and $\{\check{\mathbf{x}}_m^w\}$) will be processed to obtain the estimates $\{(\hat{d}_u^w, \hat{\vartheta}_u^w, \hat{\varphi}_u^w)\}$ of U points. Meanwhile, these estimates will be inserted into the known training signal model to update the data $\{\tilde{\mathbf{x}}_n^{w+1}\}$ and $\{\check{\mathbf{x}}_m^{w+1}\}$. This strategy aims to make the iterative data $\{\tilde{\mathbf{x}}_n^w\}$ and $\{\check{\mathbf{x}}_m^w\}$ continuously approach the complete data $\{\tilde{\mathbf{x}}_n\}$ and $\{\check{\mathbf{x}}_m\}$, ultimately obtaining estimates for U SBSs.

1) Designing Data for the w-th Iteration: At the w-th iteration, the data set $\{\tilde{\mathbf{x}}_n^w | n = 1, \ldots, N\}$ will be designed based on N columns of the observation matrix (5). Taking $\tilde{\mathbf{x}}_n^w$ as an example, it can be expressed as

$$\tilde{\mathbf{x}}_n^w = \left[\tilde{\mathbf{x}}_{n,1}^{w\,\mathrm{T}}, \tilde{\mathbf{x}}_{n,2}^{w\,\mathrm{T}}, \ldots, \tilde{\mathbf{x}}_{n,U}^{w\,\mathrm{T}}\right]^{\mathrm{T}}, \tag{10}$$

whose u-th component

$$\tilde{\mathbf{x}}_{n,u}^w = \tilde{\mathbf{a}}_{n,u}^w \tilde{s}_{n,u}^w + \tilde{\mathbf{z}}_{n,u}^w = \tilde{\mathbf{a}}_{n,u}^w \tilde{s}_{n,u}^w + \beta_u \left[\tilde{\mathbf{y}}'_n - \tilde{\mathbf{v}}_{n,u}^w\right] \tag{11}$$

embeds formally the parameters $(d_u^w, \vartheta_u^w, \varphi_u^w)$ to be estimated for a point through $\tilde{\mathbf{a}}_{n,u}^w = [e^{i\ell_1\varphi_u^w} J_{\ell_1}(k_n R_s \sin\vartheta_u^w), \ldots, e^{i\ell_M\varphi_u^w} J_{\ell_M}(k_n R_s \sin\vartheta_u^w)]^{\mathrm{T}}$ and $\tilde{s}_{n,u}^w = s_u J_0(k_n R_m \sin\vartheta_u^w) \times e^{ik_n d_u^w}/d_u^w$. Therefore, the estimated positions for U points at the w-th iteration can be obtained by sequentially processing U components in $\{\tilde{\mathbf{x}}_n^w\}$. The specific processing steps will be discussed later. Further, in (11), we specially design $\tilde{\mathbf{v}}_{n,u}^w$ in the noise component $\tilde{\mathbf{z}}_{n,u}^w$ to be the projection of the observation $\tilde{\mathbf{y}}'_n$ onto the subspace spanned by the first $(u-1)$ estimated

positions, to completely remove the component of $\tilde{\mathbf{y}}'_n$ about these estimates, thereby preventing the iterative estimation process from falling into local optima. Specifically, after obtaining the estimates $\{(\hat{d}_i, \hat{\vartheta}_i, \hat{\varphi}_i)|i = 1, \ldots, u-1\}$ by processing the first $u-1$ components in $\{\tilde{\mathbf{x}}_n^w\}$, we construct

$$\bar{\mathbf{x}}_{n,u}^w = \sum_{i=1}^{u-1} \tilde{\mathbf{a}}_{n,i}^w \tilde{s}_{n,i}^w \tag{12}$$

by substituting the estimates $\{(\hat{d}_i, \hat{\vartheta}_i, \hat{\varphi}_i)|i = 1, \ldots, u-1\}$ into the aforementioned forms of $\tilde{\mathbf{a}}_{n,i}^w$ and $\tilde{s}_{n,i}^w$, and summing them up. Then, the eigen value decomposition (EVD) of $\tilde{\mathbf{R}}_{\bar{\mathbf{x}}_{n,u}}^w = \mathbb{E}\{\bar{\mathbf{x}}_{n,u}^w (\bar{\mathbf{x}}_{n,u}^w)^{\mathrm{H}}\}$ takes the form

$$\tilde{\mathbf{R}}_{\bar{\mathbf{x}}_{n,u}}^w = \sum_{i=1}^{u-1} \tilde{\chi}_i^w \tilde{\mathbf{u}}_i^w (\tilde{\mathbf{u}}_i^w)^{\mathrm{H}} = \tilde{\mathbf{U}}_{n,u}^w \tilde{\Upsilon}_{n,u}^w \left(\tilde{\mathbf{U}}_{n,u}^w\right)^{\mathrm{H}}, \tag{13}$$

where $\tilde{\Upsilon}_{n,u}^w = \mathrm{diag}\{\tilde{\chi}_1^w, \tilde{\chi}_2^w, \ldots, \tilde{\chi}_{u-1}^w\}$ contains the non- zero eigenvalues of $\tilde{\mathbf{R}}_{\bar{\mathbf{x}}_{n,u}}^w$ arranged in descending order, and $\tilde{\mathbf{U}}_{n,u}^w = [\tilde{\mathbf{u}}_1^w, \tilde{\mathbf{u}}_2^w, \ldots, \tilde{\mathbf{u}}_{u-1}^w] \in \mathbb{C}^{M\times(u-1)}$ is composed of the corresponding eigenvectors. Subsequently, the eigenvectors $\{\tilde{\mathbf{u}}_i^w\}$ in $\tilde{\mathbf{U}}_{n,u}^w$ are utilized to update the projection operator $\tilde{\Omega}_{n,u}^w \in \mathbb{C}^{M\times U}$ as

$$\tilde{\Omega}_{n,u}^w = \left[\tilde{\mathbf{u}}_1^w, \ldots, \tilde{\mathbf{u}}_{u-1}^w, \tilde{\mathbf{u}}_u^{w-1}, \ldots, \tilde{\mathbf{u}}_U^{w-1}\right]. \tag{14}$$

It means that the first $(u-1)$ components in $\tilde{\Omega}_{n,u}^w$ are derived from the subspace spanned by the first $(u-1)$ estimated positions $\{(\hat{d}_i, \hat{\vartheta}_i, \hat{\varphi}_i)|i = 1, \ldots, u-1\}$ at the w-th iteration. Based on $\tilde{\Omega}_{n,u}^w$, the subspace projector applied to $\tilde{\mathbf{v}}_{n,u}^w$ is designed as

$$\tilde{\mathbf{P}}_{n,u}^w = \tilde{\Omega}_{n,u}^w \left[\left(\tilde{\Omega}_{n,u}^w\right)^{\mathrm{H}} \tilde{\Omega}_{n,u}^w\right]^{-1} \left(\tilde{\Omega}_{n,u}^w\right)^{\mathrm{H}}. \tag{15}$$

Finally, we construct $\tilde{\mathbf{v}}_{n,u}^w$ as $\tilde{\mathbf{v}}_{n,u}^w = \tilde{\mathbf{P}}_{n,u}^w \tilde{\mathbf{y}}'_n$.

2) Estimating $\{(\vartheta_u^w, \varphi_u^w)\}$ at the w-th Iteration: After designing $\tilde{\mathbf{v}}_{n,u}^w$, the covariance of $\tilde{\mathbf{x}}_{n,u}^w$ can be written as

$$\begin{aligned}\tilde{\mathbf{R}}_{\tilde{\mathbf{x}}_{n,u}}^w &= \mathbb{E}\left\{\tilde{\mathbf{x}}_{n,u}^w (\tilde{\mathbf{x}}_{n,u}^w)^{\mathrm{H}}\right\} \\ &= \tilde{\mathbf{a}}_{n,u}^w \mathbb{E}\{\tilde{s}_{n,u}^w (\tilde{s}_{n,u}^w)^*\} (\tilde{\mathbf{a}}_{n,u}^w)^{\mathrm{H}} + \mathbb{E}\left\{\tilde{\mathbf{z}}_{n,u}^w (\tilde{\mathbf{z}}_{n,u}^w)^{\mathrm{H}}\right\} \\ &= \tilde{\mathbf{a}}_{n,u}^w \tilde{R}_{\tilde{s}_{n,u}}^w (\tilde{\mathbf{a}}_{n,u}^w)^{\mathrm{H}} + \tilde{\mathbf{R}}_{\tilde{\mathbf{z}}_{n,u}}^w. \end{aligned} \tag{16}$$

The EVD of $\tilde{\mathbf{R}}_{\tilde{\mathbf{x}}_{n,u}}^w$ is given by

$$\tilde{\mathbf{R}}_{\tilde{\mathbf{x}}_{n,u}}^w = \sum_{m=1}^{M} \tilde{\lambda}_m^w \tilde{\mathbf{q}}_m^w (\tilde{\mathbf{q}}_m^w)^{\mathrm{H}} = \tilde{\mathbf{Q}}_{n,u}^w \tilde{\Lambda}_{n,u}^w \left(\tilde{\mathbf{Q}}_{n,u}^w\right)^{\mathrm{H}} \tag{17}$$

with $\tilde{\Lambda}_{n,u}^w = \mathrm{diag}\{\tilde{\lambda}_1^w, \tilde{\lambda}_2^w, \ldots, \tilde{\lambda}_M^w\} \in \mathbb{C}^{M\times M}$, and $\tilde{\mathbf{Q}}_{n,u}^w = [\tilde{\mathbf{q}}_1^w, \tilde{\mathbf{q}}_2^w, \ldots, \tilde{\mathbf{q}}_M^w] \in \mathbb{C}^{M\times M}$. From (16), the covariance $\tilde{\mathbf{R}}_{\bar{\mathbf{x}}_{n,u}}^w$ is obtained by adding a rank-one matrix to $\tilde{\mathbf{R}}_{\tilde{\mathbf{z}}_{n,u}}^w$, allowing (17) to be further divided as

$$\tilde{\mathbf{R}}_{\bar{\mathbf{x}}_{n,u}}^w = \tilde{\lambda}_{\max}^w \tilde{\mathbf{q}}_{\max}^w (\tilde{\mathbf{q}}_{\max}^w)^{\mathrm{H}} + \bar{\mathbf{Q}}_{n,u}^w \bar{\Lambda}_{n,u}^w (\bar{\mathbf{Q}}_{n,u}^w)^{\mathrm{H}}, \tag{18}$$

where the former corresponds to the first term in (16), consisting of the maximum eigenvalue $\lambda_{\max}^w$ and its corresponding eigenvector $\tilde{\mathbf{q}}_{\max}^w$, while the latter is spanned by the other eigenvalues and their respective eigenvectors, corresponding to $\tilde{\mathbf{R}}_{\tilde{\mathbf{z}}_{n,u}}^w$ in (16). Originating from (8), we assume the signal and noise terms in (11) to be statistical independent, so that (16) and (18) bring

$$\tilde{\mathbf{R}}_{\tilde{\mathbf{x}}_{n,u}}^w \bar{\mathbf{Q}}_{n,u}^w = \tilde{\mathbf{a}}_{n,u}^w \tilde{R}_{\tilde{s}_{n,u}}^w (\tilde{\mathbf{a}}_{n,u}^w)^{\mathrm{H}} \bar{\mathbf{Q}}_{n,u}^w + \tilde{\mathbf{R}}_{\tilde{\mathbf{z}}_{n,u}}^w \bar{\mathbf{Q}}_{n,u}^w = \tilde{\mathbf{R}}_{\tilde{\mathbf{z}}_{n,u}}^w \bar{\mathbf{Q}}_{n,u}^w, \tag{19}$$

indicating $(\tilde{\mathbf{a}}_{n,u}^w)^{\mathrm{H}} \bar{\mathbf{Q}}_{n,u}^w = 0$. Therefore, we can construct the pseudo-spectrum as

$$\tilde{P}_{n,u}^w(\vartheta, \varphi) = \frac{1}{\left(\tilde{\mathbf{a}}_{n,u}^w(\vartheta, \varphi)\right)^{\mathrm{H}} \bar{\mathbf{Q}}_{n,u}^w \left(\bar{\mathbf{Q}}_{n,u}^w\right)^{\mathrm{H}} \tilde{\mathbf{a}}_{n,u}^w(\vartheta, \varphi)}, \tag{20}$$

where $\tilde{\mathbf{a}}_{n,u}^w(\vartheta, \varphi) = [e^{i\ell_m\varphi} J_{\ell_m}(k_n R_s \sin\vartheta)]_{M\times 1}$ is the search vector on $\vartheta \in [-\pi/2, \pi/2]$ and $\varphi \in [0, 2\pi]$. The AoA $(\vartheta_u^w, \varphi_u^w)$, carried by the signal $\tilde{\mathbf{x}}_{n,u}^w$, can then be estimated by performing a 2-D spectral search on (20). Unlike the conventional MUSIC algorithm that only performs phase searching, we design a novel search vector $\tilde{\mathbf{a}}_{n,u}^w(\vartheta, \varphi)$ above. It searches for both the amplitude and phase of $\bar{\mathbf{Q}}_{n,u}^w$, thus estimating simultaneously both the azimuth angle φ_u^w carried by the exponential term $e^{i\ell_m\varphi_u^w}$ and the elevation angle ϑ_u^w embedded in the Bessel function $J_{\ell_m}(k_n R_s \sin\vartheta_u^w)$. We name this method the *amplitude-phase MUSIC* method.

Applying the AP-MUSIC method to the u-th component of each data in the data set $\{\tilde{\mathbf{x}}_n^w|n = 1, \ldots, N\}$ will result in a total of N estimates for $(\vartheta_u^w, \varphi_u^w)$, given by

$$\hat{\vartheta}_{n,u}^w = \vartheta_u^w + \tilde{\varepsilon}_{n,u}^{\vartheta}, \quad \hat{\varphi}_{n,u}^w = \varphi_u^w + \tilde{\varepsilon}_{n,u}^{\varphi}, \quad n = 1, \ldots, N, \tag{21}$$

where $\{(\tilde{\varepsilon}_{n,u}^{\vartheta}, \tilde{\varepsilon}_{n,u}^{\varphi})\}$ are the estimation errors. Assuming $\{\tilde{\varepsilon}_{n,u}^{\varphi}\}$ have the same variances $\mathrm{Var}(\tilde{\varepsilon}_u^{\varphi})$, due to $\mathrm{Var}(\frac{1}{N}\sum_{n=1}^{N} \hat{\varphi}_{n,u}^w) = \frac{\mathrm{Var}(\tilde{\varepsilon}_u^{\varphi})}{N}$, we adopt

$$\hat{\varphi}_u^w = \frac{1}{N} \sum_{n=1}^{N} \hat{\varphi}_{n,u}^w \tag{22}$$

as the estimate of φ_u^w. Using the method described above sequentially on U components of all the data in $\{\tilde{\mathbf{x}}_n^w\}$ yields the estimated azimuth angles $\{\hat{\varphi}_u^w\}$ for U points at the w-th iteration.

3) Estimating $\{(d_u^w, \vartheta_u^w)\}$ at the w-th Iteration: When estimating $\{(d_u^w, \vartheta_u^w)\}$ in the frequency domain, the data set $\{\check{\mathbf{x}}_m^w|m = 1, \ldots, M\}$ at the w-th iteration will be designed based on M rows of the observation matrix (5), and the data $\check{\mathbf{x}}_m^w$ can be similarly expressed as

$$\check{\mathbf{x}}_m^w = \left[\check{\mathbf{x}}_{m,1}^{w\,\mathrm{T}}, \check{\mathbf{x}}_{m,2}^{w\,\mathrm{T}}, \ldots, \check{\mathbf{x}}_{m,U}^{w\,\mathrm{T}}\right]^{\mathrm{T}}, \tag{23}$$

with the u-th component

$$\check{\mathbf{x}}_{m,u}^w = \check{\mathbf{b}}_{m,u}^w \check{s}_{m,u}^w + \beta'_u\left[\check{\mathbf{y}}'_m - \check{\mathbf{v}}_{m,u}^w\right], \tag{24}$$

where $\check{\mathbf{b}}_{m,u}^w = [e^{ik_1 d_u^w} J_{\ell_m}(k_1 R_s \sin\vartheta_u^w) J_{\ell_0}(k_1 R_m \sin\vartheta_u^w), , \ldots, e^{ik_N d_u^w} J_{\ell_m}(k_N R_s \sin\vartheta_u^w) J_{\ell_0}(k_N R_m \sin\vartheta_u^w)]^{\mathrm{T}}$, $\check{s}_{m,u}^w = s_u e^{i\ell_m\varphi_u^w}/d_u^w$, $\check{\mathbf{y}}'_m$ is the m-th row in (5), and $\check{\mathbf{v}}_{m,u}^w$ is designed using a similar method from (12) to (15). Then, following the AP-MUSIC approach, we can obtain $\{(\hat{d}_{m,u}^w, \hat{\vartheta}_{m,u}^w)|u = 1,, \ldots, U;\ m = 1,, \ldots, M\}$, and eventually we have

$$\begin{cases} \hat{\vartheta}_u^w = \frac{1}{M+N}\left(\sum_{m=1}^{M} \hat{\vartheta}_{m,u}^w + \sum_{n=1}^{N} \hat{\vartheta}_{n,u}^w\right), \\ \hat{d}_u^w = \frac{1}{M}\sum_{m=1}^{M} \hat{d}_{m,u}^w, \quad u = 1, \ldots, U. \end{cases} \tag{25}$$

Thus, the estimated positions $\{(\hat{d}_u^w, \hat{\vartheta}_u^w, \hat{\varphi}_u^w)\}$ of U points at the w-th iteration have been obtained.

4) Loop Iteration: After completing the estimation for the data $\{\tilde{\mathbf{x}}_n^w\}$ and $\{\check{\mathbf{x}}_m^w\}$ at the w-th iteration, the data for the $(w+1)$-th iteration are updated as

$$\begin{cases} \tilde{\mathbf{x}}_n^{w+1} = \left[\tilde{\mathbf{x}}_{n,1}^{w+1\mathrm{T}}, \ldots, \tilde{\mathbf{x}}_{n,U}^{w+1\mathrm{T}}\right]^{\mathrm{T}}, \ n = 1, \ldots, N, \\ \check{\mathbf{x}}_m^{w+1} = \left[\check{\mathbf{x}}_{m,1}^{w+1\mathrm{T}}, \ldots, \check{\mathbf{x}}_{m,U}^{w+1\mathrm{T}}\right]^{\mathrm{T}}, \ m = 1, \ldots, M, \end{cases} \tag{26}$$

where their u-th components are iteratively calculated as

$$\begin{cases} \tilde{\mathbf{x}}_{n,u}^{w+1} = \tilde{\mathbf{a}}_{n,u}^{w+1} \tilde{s}_{n,u}^{w+1} + \beta_u \left[\tilde{\mathbf{y}}_n' - \tilde{\mathbf{v}}_{n,u}^{w+1}\right], \\ \check{\mathbf{x}}_{m,u}^{w+1} = \check{\mathbf{b}}_{m,u}^{w+1} \check{s}_{m,u}^{w+1} + \beta_u' \left[\check{\mathbf{y}}_m' - \check{\mathbf{v}}_{m,u}^{w+1}\right], \end{cases} \tag{27}$$

by substituting the estimates $\{(\hat{d}_u^w, \hat{\vartheta}_u^w, \hat{\varphi}_u^w)\}$ from the w-th iteration into the aforementioned forms of $\tilde{\mathbf{a}}_{n,u}^w$ and $\tilde{s}_{n,u}^w$, or $\check{\mathbf{b}}_{m,u}^w$ and $\check{s}_{m,u}^w$. Then, the previously mentioned subspace projection method would be used to design $\{\tilde{\mathbf{v}}_{n,u}^{w+1}, \check{\mathbf{v}}_{m,u}^{w+1}\}$, and the AP-MUSIC method would be used to update the estimated positions $\{(\hat{d}_u^{w+1}, \hat{\vartheta}_u^{w+1}, \hat{\varphi}_u^{w+1})\}$ of U points. The entire iterative estimation process will continue until

$$\begin{cases} \sum_{n=1}^{N} \|\tilde{\mathbf{y}}_n' - \sum_{i=1}^{U} \tilde{\mathbf{a}}_{n,i}^w \tilde{s}_{n,i}^w\| \le \xi_{\text{mode}}, \\ \sum_{m=1}^{M} \|\check{\mathbf{y}}_m' - \sum_{i=1}^{U} \check{\mathbf{b}}_{m,i}^w \check{s}_{m,i}^w\| \le \xi_{\text{freq}}, \end{cases} \tag{28}$$

where $\|\cdot\|$ is the Euclidean norm, ξ_{mode} and ξ_{freq} are the iteration termination conditions in the OAM mode and frequency domains, respectively, designed based on the signal-to-noise ratio (SNR) at the MBS. The specific steps to obtain U SBS estimated positions using the proposed iterative estimation method are summarized in Algorithm 1.

C. Pilot Overhead and Computational Complexity

In the following, we will analyze the pilot overhead and computational complexity required for the proposed iterative estimation method that multiplexes M OAM modes and N subcarriers. Due to the use of the iterative estimation strategy, the observations $\{\tilde{\mathbf{y}}_n'\}$ (and also $\{\check{\mathbf{y}}_m'\}$) can be decomposed into $\{\tilde{\mathbf{x}}_n^w\}$ (and $\{\check{\mathbf{x}}_m^w\}$) containing U independent components, thereby enabling the independent estimation for the positions of U SBSs. This eliminates the mandatory requirement for $\{\tilde{\mathbf{y}}_n'\}$ and $\{\check{\mathbf{y}}_m'\}$ to be non-coherent observations. Therefore, during the training phase, the channel uses on each mode and each subcarrier is reduced from $L \ge U$, as required by the existing algorithm [11], to $L = 1$. In other words, the total channel uses required by the MBS during the training phase is reduced from MNU to MN, significantly saving the pilot overhead.

However, the loop iterative strategy may result in a high computational complexity, which is evaluated in Table I. Taking the estimation within the OAM mode domain as an example, the computational complexity in designing $\{\tilde{\mathbf{v}}_{n,u}^w\}$ mainly originates from the EVD for $\{\tilde{\mathbf{R}}_{\tilde{\mathbf{x}}_{n,u}}^w\}$ and the calculation of $\{\tilde{\mathbf{P}}_{n,u}^w\}$, with complexities of $\mathcal{O}(UNM^3)$ and $\mathcal{O}(UNM^3 + U^2NM^2 + U^3NM)$ respectively. Subsequently, the complexity of executing the AP-MUSIC algorithm on $\{\tilde{\mathbf{x}}_{n,u}^w\}$ is determined by computing the covariances $\{\tilde{\mathbf{R}}_{\tilde{\mathbf{x}}_{n,u}}^w\}$ and performing EVD on $\{\tilde{\mathbf{R}}_{\tilde{\mathbf{x}}_{n,u}}^w\}$, corresponding to complexities $\mathcal{O}(UNM^2)$ and $\mathcal{O}(UNM^3)$. The computational complexity in the frequency domain is similarly summarized in Table I. Ultimately, the complexity of the proposed iterative estimation algorithm in each iteration is $\mathcal{O}(UMN^3 + UNM^3 + U^3MN + U^2NM^2 + U^2MN^2)$, determined by the number of SBSs U, and the number of multiplexed OAM modes M and subcarriers N.

Algorithm 1 Iterative Estimation to Obtain $\{(d_u, \vartheta_u, \varphi_u)\}$

Input: $\mathbf{Y}' = [y'(\ell_m, k_n)]_{M\times N}$, ξ_{mode}, ξ_{freq} and U
Output: $\{(\hat{d}_u, \hat{\vartheta}_u, \hat{\varphi}_u) | u = 1, \ldots, U\}$

Init.: initialize $w = 0$, and arbitrarily assume the positions of U points to form $\{\tilde{\mathbf{x}}_n^w\}$ and $\{\check{\mathbf{x}}_m^w\}$ as in (10) and (23);
while $\sum_{n=1}^{N} \|\tilde{\mathbf{y}}_n' - \sum_{i=1}^{U} \tilde{\mathbf{a}}_{n,i}^w \tilde{s}_{n,i}^w\| > \xi_{\text{mode}}$ or $\sum_{m=1}^{M} \|\check{\mathbf{y}}_m' - \sum_{i=1}^{U} \check{\mathbf{b}}_{m,i}^w \check{s}_{m,i}^w\| > \xi_{\text{freq}}$
  $w = w + 1$;
  for $u = 1{:}U$
    for $n = 1{:}N$
      $\tilde{\mathbf{v}}_{n,u}^w \leftarrow \tilde{\mathbf{P}}_{n,u}^w \tilde{\mathbf{y}}_n'$ according to (12) to (15);
      $\tilde{\mathbf{x}}_{n,u}^w \leftarrow \tilde{\mathbf{a}}_{n,u}^w \tilde{s}_{n,u}^w + \beta_u \left[\tilde{\mathbf{y}}_n' - \tilde{\mathbf{v}}_{n,u}^w\right]$;
      $\tilde{\mathbf{R}}_{\tilde{\mathbf{x}}_{n,u}}^w \leftarrow \mathbb{E}\{\tilde{\mathbf{x}}_{n,u}^w (\tilde{\mathbf{x}}_{n,u}^w)^{\mathrm{H}}\}$;
      $\tilde{\mathbf{Q}}_{n,u}^w$, $\tilde{\Lambda}_{n,u}^w \leftarrow$ decompose $\tilde{\mathbf{R}}_{\tilde{\mathbf{x}}_{n,u}}^w$ according to (17);
      $\tilde{\Lambda}_{n,u}^w \leftarrow \mathrm{diag}\{\tilde{\lambda}_1^w, \tilde{\lambda}_2^w, \ldots, \tilde{\lambda}_M^w\}$, $\tilde{\lambda}_1^w \ge \cdots \ge \tilde{\lambda}_M^w$;
      $\bar{\Lambda}_{n,u}^w \leftarrow \mathrm{diag}\{\tilde{\lambda}_2^w, \cdots, \tilde{\lambda}_M^w\}$;
      $\bar{\mathbf{Q}}_{n,u}^w \leftarrow$ the columns in $\tilde{\mathbf{Q}}_{n,u}^w$ corresponding to $\bar{\Lambda}_{n,u}^w$;
      $\tilde{\mathbf{a}}_{n,u}^w(\vartheta, \varphi) \leftarrow [e^{i\ell_m\varphi} J_{\ell_m}(k_n R_s \sin\vartheta)]_{M\times 1}$;
      $\tilde{P}_{n,u}^w(\vartheta, \varphi) \leftarrow \frac{1}{(\tilde{\mathbf{a}}_{n,u}^w(\vartheta,\varphi))^{\mathrm{H}} \bar{\mathbf{Q}}_{n,u}^w (\bar{\mathbf{Q}}_{n,u}^w)^{\mathrm{H}} \tilde{\mathbf{a}}_{n,u}^w(\vartheta,\varphi)}$;
      $(\hat{\vartheta}_{n,u}^w, \hat{\varphi}_{n,u}^w) \leftarrow$ 2-D spectral search on $\tilde{P}_{n,u}^w(\vartheta, \varphi)$;
    end for
    for $m = 1{:}M$
      $(\hat{d}_{m,u}^w, \hat{\vartheta}_{m,u}^w) \leftarrow$ execute the AP-MUSIC method, as in steps 5 - 16;
    end for
    $\hat{d}_u^w \leftarrow \frac{1}{M} \sum_{m=1}^{M} \hat{d}_{m,u}^w$;
    $\hat{\vartheta}_u^w \leftarrow \frac{1}{M+N} \left(\sum_{m=1}^{M} \hat{\vartheta}_{m,u}^w + \sum_{n=1}^{N} \hat{\vartheta}_{n,u}^w\right)$;
    $\hat{\varphi}_u^w \leftarrow \frac{1}{N} \sum_{n=1}^{N} \hat{\varphi}_{n,u}^w$;
  end for
end while
$(\hat{d}_u, \hat{\vartheta}_u, \hat{\varphi}_u) \leftarrow (\hat{d}_u^w, \hat{\vartheta}_u^w, \hat{\varphi}_u^w)$, $u = 1, \ldots, U$.
end procedure

TABLE I
THE COMPLEXITY OF ITERATIVE ESTIMATION ALGORITHM

Domain	Main Steps		Complexity
OAM Mode	Design $\{\tilde{\mathbf{v}}_{n,u}^w\}$	$\{\tilde{\mathbf{R}}_{\tilde{\mathbf{x}}_{n,u}}^w\}$	$\mathcal{O}(UNM^3)$
		$\{\tilde{\mathbf{P}}_{n,u}^w\}$	$\mathcal{O}(UNM^3 + U^2NM^2 + U^3NM)$
	AP-MUSIC	$\{\tilde{\mathbf{R}}_{\tilde{\mathbf{x}}_{n,u}}^w\}$	$\mathcal{O}(UNM^2)$
		EVD for $\{\tilde{\mathbf{R}}_{\tilde{\mathbf{x}}_{n,u}}^w\}$	$\mathcal{O}(UNM^3)$
Frequency	Design $\{\check{\mathbf{v}}_{m,u}^w\}$	$\{\check{\mathbf{R}}_{\check{\mathbf{x}}_{m,u}}^w\}$	$\mathcal{O}(UMN^3)$
		$\{\check{\mathbf{P}}_{m,u}^w\}$	$\mathcal{O}(UMN^3 + U^2MN^2 + U^3MN)$
	AP-MUSIC	$\{\check{\mathbf{R}}_{\check{\mathbf{x}}_{m,u}}^w\}$	$\mathcal{O}(UMN^2)$
		EVD for $\{\check{\mathbf{R}}_{\check{\mathbf{x}}_{m,u}}^w\}$	$\mathcal{O}(UMN^3)$
The total complexity: $\mathcal{O}(UMN^3 + UNM^3 + U^3MN + U^2NM^2 + U^2MN^2)$			

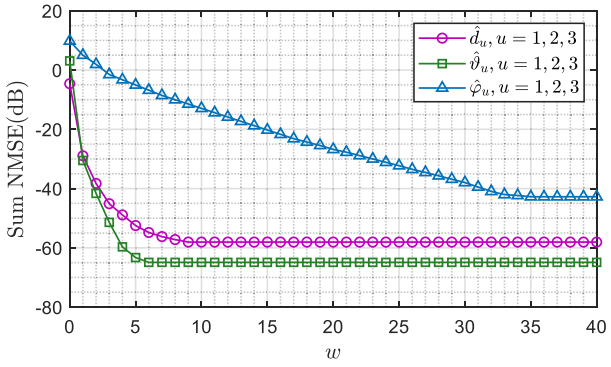

Fig. 2. The sum NMSEs vs. w for the proposed approach.

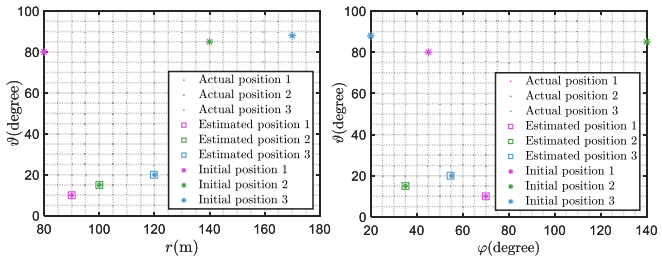

Fig. 3. The estimated positions of SBSs.

IV. Numerical Results

In the following, the numerical results are given to assess the performance of the proposed iterative estimation method. We choose to multiplex $M = 11$ OAM modes ranging from $\ell = -5, -4, \ldots, +5$, and 33 subcarriers corresponding to $k = 56, 57, \ldots, 88$. The SBS UCAs are configured with $Q = 11$ elements each, having a radius of $R_s = 10\lambda$, and there are $U = 3$ SBSs. The UCA at the MBS comprises $P = 33$ elements, with a radius of $R_m = 10\lambda$, where $\lambda = 2\pi/k_1$, and $k_1 = 56$. The SBSs are positioned at O_1(90m, 10°, 70°), O_2(100m, 15°, 35°) and O_3(120m, 20°, 55°). In Algorithm 1, the initial positions of $U = 3$ points are set at (80m, 80°, 45°), (140m, 85°, 140°) and (170m, 88°, 20°).

Fig. 2 illustrates the sum normalized mean squared error (NMSE) as a function of the iteration count w at SNR = 20 dB, using the iterative estimation method integrated with AP-MUSIC. The sum NMSE is defined as $\sum_u \mathbb{E}\{(\hat{a}_u - a_u)^2/a_u^2\}$, where $\hat{a}_u$ is the estimate of a_u. As anticipated, the proposed iterative estimation method exhibits progressive convergence with increasing w. Additionally, due to the limited number of UCA elements at the SBS, the number of multiplexed OAM modes is fewer than the utilized subcarriers, resulting in slower convergence and higher estimation error for the azimuth angle $\{\hat{\varphi}_u\}$ estimated within the OAM mode domain.

Fig. 3 presents an intuitive example of the estimated positions of the SBSs obtained at SNR = 20 dB, after $w = 40$ iterations. Utilizing the proposed iterative estimation method, the estimated positions, located at $\hat{\mathrm{O}}_1$ (90.00m, 10.00°, 70.00°), $\hat{\mathrm{O}}_2$ (100.00m, 15.00°, 35.00°) and $\hat{\mathrm{O}}_3$ (119.85m, 20.00°, 54.60°), are almost precisely at the actual positions of the SBSs, thereby intuitively demonstrating the effectiveness of the proposed method.

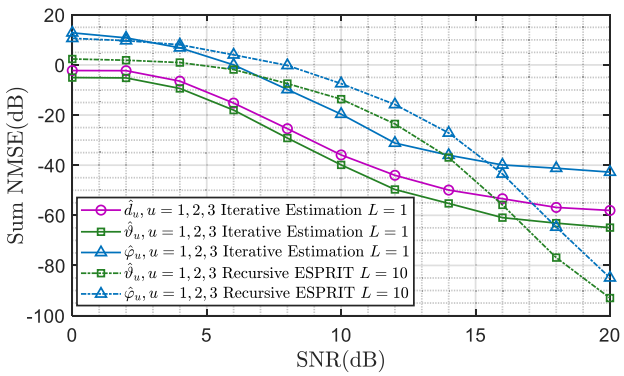

Fig. 4. The sum NMSEs vs. SNR for different approaches.

Fig. 4 depicts the sum NMSE of the iterative estimation method as a function of SNR. For comparative purposes, we also include the sum NMSE for azimuth and elevation angles, estimated using the recursive ESPRIT algorithm from [11]. As discussed in Section III-C, to ensure the non-coherent observations within the OAM mode domain, in the MU-OAM system utilizing the recursive ESPRIT [11], all the SBSs sequentially transmit $L = 10$ pilot signals on each OAM mode. While for the proposed iterative estimation method, as depicted in Algorithm 1, SBSs only transmit $L = 1$ training signal on each OAM mode and/or subcarrier. From Fig. 4, the proposed method matches the accuracy of the recursive ESPRIT in estimating azimuth and elevation angles while requiring fewer training overhead. Additionally, it precisely estimates distances between the MBS and SBSs, thereby contributing to the acquisition of complete and precise CSI.

V. Conclusion

In this paper, we propose an iterative estimation method based on the AP-MUSIC algorithm to precisely locate all SBSs. This method reduces training overhead by $1/U$ compared to existing alternatives by obviating the need for continuous transmission of training signals on the multiplexed OAM modes and subcarriers. Furthermore, it ensures precise estimation of the distances between the MBS and SBSs, while maintaining comparable accuracy in azimuth and elevation angle estimations to current methods, facilitating the acquisition of complete and accurate CSI. Numerical results demonstrated the effectiveness of the proposed solution compared to existing alternatives.

References

[1] S. Yang, C. Xu, L. Zhong, J. Shen, and G.-M. Muntean, "A QoE-driven multicast strategy with segment routing—A novel multimedia traffic engineering paradigm," *IEEE Trans. Broadcast.*, vol. 66, no. 1, pp. 34–46, Mar. 2020.

[2] H. Jung et al., "Feasibility verification of ATSC 3.0 MIMO system for 8K-UHD terrestrial broadcasting," *IEEE Trans. Broadcast.*, vol. 67, no. 4, pp. 909–916, Dec. 2021.

[3] J. Xiong, Y. Fang, P. Cheng, Z. Shi, and W. Zhang, "Distributed caching in converged networks: A deep reinforcement learning approach," *IEEE Trans. Broadcast.*, vol. 67, no. 1, pp. 201–211, Mar. 2021.

[4] W. Wu et al., "AI-native network slicing for 6G networks," *IEEE Wireless Commun.*, vol. 29, no. 1, pp. 96–103, Feb. 2022.

[5] H. H. Yang, G. Geraci, and T. Q. S. Quek, "Energy-efficient design of MIMO heterogeneous networks with wireless backhaul," *IEEE Trans. Wireless Commun.*, vol. 15, no. 7, pp. 4914–4927, Jul. 2016.

[6] N. Wang, E. Hossain, and V. K. Bhargava, "Backhauling 5G small cells: A radio resource management perspective," *IEEE Wireless Commun.*, vol. 22, no. 5, pp. 41–49, Oct. 2015.

[7] U. Siddique, H. Tabassum, E. Hossain, and D. I. Kim, "Wireless backhauling of 5G small cells: Challenges and solution approaches," *IEEE Wireless Commun.*, vol. 22, no. 5, pp. 22–31, Oct. 2015.

[8] R. Chen, J. Lin, B. Zhang, Y. Ding, and K. Xu, "Precoding-based downlink OAM-MIMO communications with rate splitting," *IEEE Trans. Broadcast.*, vol. 69, no. 4, pp. 894–903, Dec. 2023.

[9] W.-X. Long, R. Chen, M. Moretti, J. Xiong, and J. Li, "Joint spatial division and coaxial multiplexing for downlink multi-user OAM wireless backhaul," *IEEE Trans. Broadcast.*, vol. 67, no. 4, pp. 879–893, Dec. 2021.

[10] R. Chen, W.-X. Long, X. Wang, and L. Jiandong, "Multi-mode OAM radio waves: Generation, angle of arrival estimation and reception with UCAs," *IEEE Trans. Wireless Commun.*, vol. 19, no. 10, pp. 6932–6947, Oct. 2020.

[11] W.-X. Long, R. Chen, and M. Moretti, "Recursive ESPRIT algorithm for multi-user OAM low-overhead AoA estimation," *IEEE Trans. Veh. Technol.*, vol. 72, no. 2, pp. 2672–2677, Feb. 2023.

[12] R. Schmidt, "Multiple emitter location and signal parameter estimation," *IEEE Trans. Antennas Propag.*, vol. 34, no. 3, pp. 276–280, Mar. 1986.

[13] W.-X. Long, R. Chen, M. Moretti, W. Zhang, and J. Li, "Joint OAM radar-communication systems: Target recognition and beam optimization," *IEEE Trans. Wireless Commun.*, vol. 22, no. 7, pp. 4327–4341, Jul. 2023.

[14] M. Feder and E. Weinstein, "Parameter estimation of superimposed signals using the EM algorithm," *IEEE Trans. Acoust., Speech, Signal Process.*, vol. 36, no. 4, pp. 477–489, Apr. 1988.